

OPTICAL TRAPS

PACS numbers: 42.50.Wk; 42.79.Kr
DOI: 10.1070/QE2014v044n12ABEH015598

Formation of contour optical traps using a four-channel liquid crystal focusing device

A.V. Korobtsov, S.P. Kotova, N.N. Losevsky, A.M. Mayorova, S.A. Samagin

Abstract. **The capabilities and specific features of the formation and dynamic control of so-called contour optical traps using a four-channel liquid crystal modulator are studied theoretically and experimentally. Circular, elliptical and C-shaped traps are formed. Trapping and confinement of absorbing micro-objects by the formed traps are demonstrated.**

Keywords: *optical traps, micro-objects, dynamic manipulation, liquid-crystal modulators, absorbing particles.*

1. Introduction

The use of multipixel phase liquid-crystal (LC) space–time light modulators (STLMs) in the schemes of optical tweezers made it possible to considerably extend the laser manipulation capabilities. Providing the possibility of real-time control of the spatial characteristics of light fields with maximum intensities up to several watts per square centimetre, the LC STLMs are widely used for the formation and transformation of arrays of differently shaped light traps [1–3], as well as for the formation of light traps of complex configurations, including those with a vortex component [4–6]. As a rule, the technology of production and control of these modulators is rather complicated, because of which they are rather expensive. At the same time, the use of such phase modulators for solving some practically important problems is excessive. In [7–9], we proposed and studied a so-called LC focusing device (or a four-channel LC modulator) based on crossed substrates of cylindrical modal lenses. This LC modulator has less controlling contacts (as little as four) than commercial modulators, which reduces its capabilities in the formation of light fields. However, this modulator has sufficient functional ability, high energy efficiency and a wider working spectral range, while the considerably simpler design and controlling system make it much less expensive. The LC focusing device makes it possible to form point optical traps with a controllable position in the manipulation plain and traps in the form of a light segment with a desired orientation. Experiments on the application of the LC focusing device in an optical tweezers scheme are described in [10]. We demonstrated transfer of a transparent dielectric micro-object along a given square trajectory by a point trap, as well as simultaneous trapping of several particles and their rotation by a trap in the form of a segment. Thus, it is shown that, for some practically important problems, the LC focusing device can be an inexpensive, technologically simple and compact alternative to commercial multipixel spatial light modulators.

In the present work, we consider the possibility of using the LC focusing device for the formation of light traps in the form of circles with the minimal intensity in their centres. Interest to optical traps of this form is related first of all to the possibility of trapping nontransparent objects or objects whose refractive index is lower than that of the environment, as well as to the problem of minimisation of the effect of radiation on the trapped objects. These features are interesting for biomedical investigations and for problems of micromechanics.

The methods of formation of intensity distributions in the form of light circles are well known and rather diversified. These distributions are typical for higher-order Laguerre–Gaussian modes [11–13], as well as for Bessel [14–17] and Airy beams [18–20]. Similar light beams can be formed by astigmatic transformations and interference methods using axicons or phase diffractive optical elements (DOEs). There are experimental studies of optical manipulation with the use of traps in the form of light circles created by both stationary DOEs [21] and LC STLMs [6, 22]. Nevertheless, from the viewpoint of using these traps for biomedical and micromechanical applications, it seems important to create compact and inexpensive optical manipulation systems. This raises the problem of investigating the possibility of the formation and control of such light traps by a tunable LC focusing device.

2. Principle of operation of LC focusing device

The principle of operation of an LC focusing device was previously described by us in [7–10]. This device consists of two crossed substrates of cylindrical modal LC lenses (Fig. 1a). The substrates were coated with transparent high-resistivity (surface resistance from 100 $k\Omega\,\square^{-1}$ to a few $M\Omega\,\square^{-1}$) films and nontransparent low-resistivity stripe contacts. The substrates were oriented so that their contact electrodes were orthogonal. The geometry of the contacts on the top and bottom layers with the notations of amplitudes and phases of applied potentials is presented in Fig. 1b. The thickness of the nematic LC layer between the substrates is given by spacers, while its initial planar orientation is determined by orienting

A.V. Korobtsov, N.N. Losevsky, S.A. Samagin Samara Branch of P.N. Lebedev Physics Institute, Russian Academy of Sciences, Novo-Sadovaya ul. 221, 443011 Samara, Russia;
e-mail: korobtsov82@gmail.com;
S.P. Kotova, A.M. Mayorova Samara Branch of P.N. Lebedev Physics Institute, Russian Academy of Sciences, Novo-Sadovaya ul. 221, 443011 Samara, Russia; Samara Aerospace State University, Moskovskoe shosse 34, 443086 Samara, Russia;
e-mail: kotova@fian.smr.ru

Received 25 June 2014; revision received 3 September 2014
Kvantovaya Elektronika **44** (12) 1157–1164 (2014)
Translated by M.N. Basieva

coatings deposited in the substrates. As was shown in [7–9], the practically interesting phase delay distributions can be obtained in the operation regime with a small modal parameter, when the effect of frequency on the voltage distribution becomes negligibly small and this distribution is controlled by the potential amplitude and phase. In this case, the equipotential lines of the voltage distribution can be only elliptical or parabolic. The voltage distributions with elliptical, circular and straight lines form phase profiles in the form of elliptic and circular cones, as well as cylindrical lens surfaces. Changing the amplitude and/or phase of potentials applied to the contacts, one can control the positions of the centres of the bases of circular and elliptic cones, the orientation of the axes of the elliptic cone and its eccentricity. These phase delays allow implementation of optical point traps with controlled positions in the manipulation plane [10], traps in the form of segments with a given orientation [10] and so-called contour light traps in the form of circles and ellipses, whose formation will be considered below.

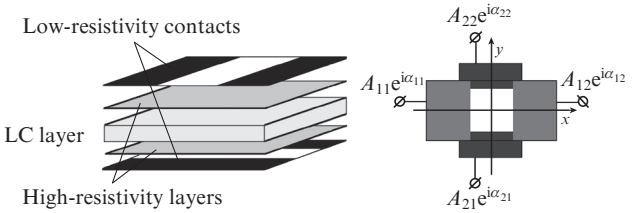

Figure 1. Schematic diagram of LC focusing device (a) and geometry of contact electrodes (b). A_{11}, A_{12}, α_{11}, α_{12} and A_{21}, A_{22}, α_{21}, α_{22} are the amplitudes and phases of voltages applied to the contact electrodes of the upper and lower layers, respectively.

For experimental formation of light fields, we used the samples of tunable LC focusing devices with square apertures with a side length of 1 mm. The high-resistivity coatings on both substrates had surface resistances of 100 kΩ $\square^{-1}$ each. The planar orientation of the LC layer (BL037, Merck) was formed with the use of orienting coatings; the LC layer thickness of 10 μm was set by Teflon spacers. The used LC layer type determines the spectral range of light modulation. In our case, it includes the visible and IR regions.

The LC focusing device was controlled by a special computer-aided quad-channel sine-wave generator [8]. The control potential frequency was 500 Hz.

3. Formation of contour traps

3.1. Formation of circular traps

Previously [7, 9], we considered different operation regimes of the LC focusing device. To form contour traps, it is convenient to use the case when the phase delay profile of the tunable LC focusing device has the form of a conical surface. To implement this phase transmission, we will consider the practically simplest control regime with a fixed potential phase shift. In this control regime, potentials φ with the phase difference π must be applied to the contacts of each of the substrates, so that the potential phases at different substrates differ by π/2: $\varphi_{11} = A_{11}e^0 = A_{11}$, $\varphi_{12} = A_{12}e^{i\pi} = -A_{12}$, $\varphi_{21} = A_{21}e^{i(3\pi/2)} = -iA_{21}$, $\varphi_{22} = A_{22}e^{i(\pi/2)} = iA_{22}$.

In this case, the potential amplitudes are related by specific relations and are the functions of the potential amplitude at one of the contacts (for example, A_{11}), of the coordinates (x_0, y_0) of the centres of the system of circles of or ellipses, and of the ratio between the lengths of the axes (γ). The voltage distribution shape and, hence, the phase delay profile are determined by the potential amplitudes. For the particular case of the square aperture and $\gamma = 1$, the equipotential lines of the voltage distribution formed at identical amplitudes of all potentials have the form of concentric circles with a centre at the point with coordinates (0, 0). The potentials corresponding to the formation of a circular trap are presented in Table 1. Due to the threshold character of the voltage–phase dependence of LC samples, the phase delay profile has a shape of a truncated cone. This is clearly demonstrated in Fig. 2, which shows the voltage and phase delay distributions over the focusing device aperture at the potentials presented in Table 1. The phase delay was visualised in the experiment using a scheme with crossed polaroids (polarisation interferometer) by a method typical for LC elements. We obtained good agreement between the calculated and experimental polarisation interference patterns.

Table 1. Potential amplitudes and phases for the formation of a circular light trap.

A_{11}/V	α_{11}/deg	A_{12}/V	α_{12}/deg	A_{21}/V	α_{21}/deg	A_{22}/V	α_{22}/deg
2	0	2	180	2	90	2	270

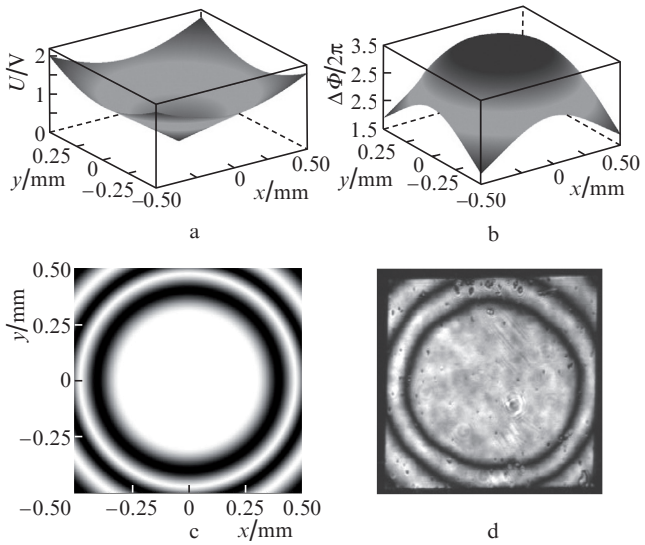

Figure 2. Voltage (a) and phase delay (b) distributions over the focusing device aperture at potentials given in Table 1, as well as calculated (c) and experimental (d) polarisation interference patterns for this case.

Optical transparency with such a phase transmission affects a homogeneous plane light wave as follows. The field intensity distribution in the far-field *xoy* plane (perpendicular to the light propagation direction) has a central maximum and additional maxima in the form of a system of concentric circles [8]. In the Fresnel diffraction region at a small distance from the LC focusing device, the light field intensity distribution has the form of a bright circle, i.e., the points with the maximal intensity lie on a curve replicating the shape of equipotential voltage lines. We used this circumstance to form contour traps of different forms. Figure 3 (upper row) shows

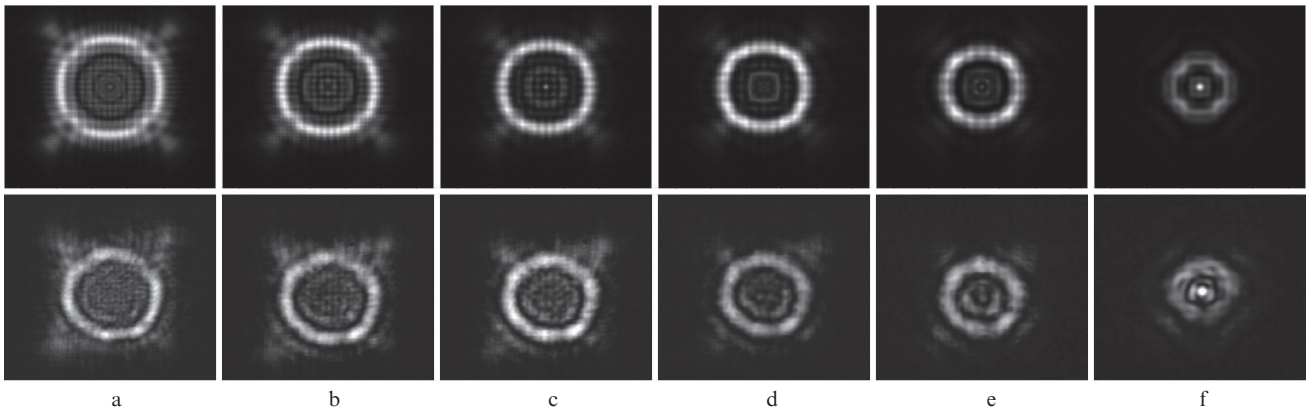

Figure 3. Calculated (upper row) and measured (lower row) light intensity distributions at potential amplitudes of 2 V at distances of 2.5 (a), 3.0 (b), 3.5 (c), 4 (d), 5 (e) and 7 cm (f).

the light intensity distributions in different planes calculated in the Fresnel approximation using the fast Fourier transform. The aperture in all the model calculations was taken to be square with a side length of 1 mm. The calculated light intensity distributions are presented in the lower row in Fig. 3.

The presented intensity distributions clearly demonstrate that, applying potentials with particular relations between their amplitudes and phases to the contacts of the LC focusing device, it is possible to create its phase delay distributions in the form of a truncated cone and, hence, to form light circles in different planes. The circle sizes decrease with increasing distance from the focusing device, and, in a particular plane, the intensity distribution becomes focused into a point. In this case both the size of the formed light circles and the range of distances from the focusing device to the circular trap formation plane are determined by the sizes and shapes of the conical surface of the phase delay. The smaller the cone angle, the smaller the distance between the focusing device and the formed circle and thereby the smaller the circle radius and the faster the transformation from a circle to a point. The conical phase delay profile dimensions can be controlled by changing the potentials at the contacts.

3.2. Formation of elliptical traps

The method considered above also makes it possible to obtain contour light traps in the form of ellipses. For the formation of these traps, the phase delay profile must have the form of truncated elliptical cone. This can be achieved by creating elliptical equipotential voltage lines in the region of the focusing device aperture and, therefore, to obtain phase delay in the form of an elliptical cone. In the considered control regime with a stationary phase shift, the amplitudes of potentials applied to different substrates must not coincide ($A_{11} \neq A_{21}$), being at the same time identical at each of the substrates ($A_{11} = A_{12}$, $A_{21} = A_{22}$). The requirements to the phase difference are the same as in the case of circular traps, i.e., the phase difference at each of the substrates must be equal to π and the potential phases at different substrates must differ by $\pi/2$ (see Table 2 and the corresponding calculated and experimental interference patterns in Fig. 4).

Similar to the case of a circular trap, the dimensions of ellipses depend on the distance to the focusing device. However, since the wavefront curvatures are different for the waves passed through the LC focusing device along the $0y$ and $0x$ axes, the intensity distribution changes faster than in the case of a circle.

Table 2. Potential amplitudes and phases for the formation of an elliptical light trap.

A_{11}/V	α_{11}/deg	A_{12}/V	α_{12}/deg	A_{21}/V	α_{21}/deg	A_{22}/V	α_{22}/deg
2	0	2	180	3	90	3	270

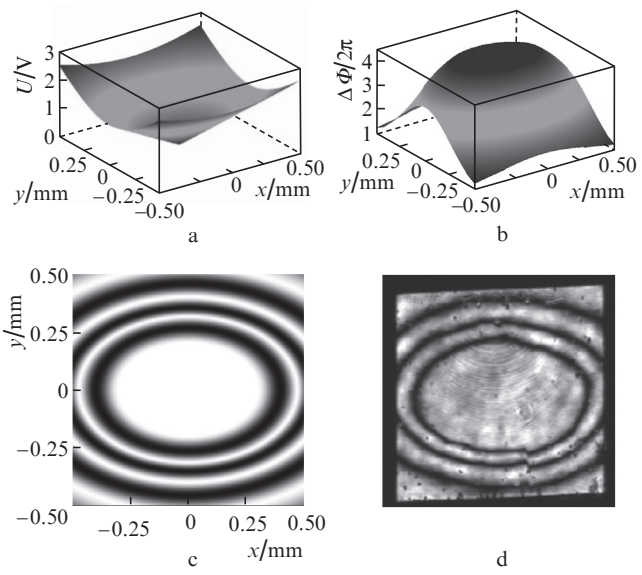

Figure 4. Voltage (a) and phase delay (b) distributions over the focusing device aperture at potentials given in Table 2, as well as calculated (c) and experimental (d) polarisation interference patterns for this case.

3.3. Formation of C-shaped traps

In [23], it was shown that crescent-shaped traps are rather effective for trapping biological objects and have some advantages compared to point traps. The LC focusing device provides the possibility of forming and controlling such traps, which opens new possibilities for optical manipulation.

To create traps in the form of circular or elliptical segments, the constant-phase lines of the phase delay distribution must be unclosed within the aperture (i.e., must have the shape of circular of elliptical segments). Then, the points of

the maximum intensity in the light field intensity distribution in the region close to the focusing device will lie on a similar curve, i.e., the field intensity distribution will have the form of a circular or elliptical segment. We will call such traps C-shaped. Unclosed constant-phase lines can be obtained, for example, due to the formation of the phase profile in the form of an elliptical cone with a base larger than the aperture. An example of such a trap is shown in Fig. 5. This trap can capture and confine objects minimising their irradiation.

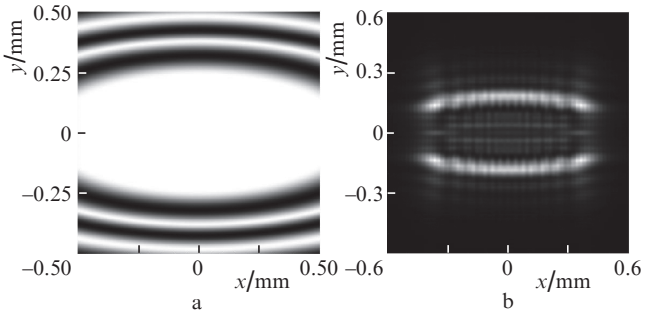

Figure 5. Polarisation interference pattern (a) and intensity distribution at a distance of 3 cm from the LC focusing device (b); potential amplitudes at the contacts are $A_{11} = A_{12} = 1$ V, $A_{21} = A_{22} = 2.5$ V.

Another method of formation of open constant-phase lines uses a shift of the centre of circular or elliptical cones. If the voltage distribution is shifted so that the constant-phase lines of the phase delay profile becomes unclosed within the aperture, then a C-shaped trap is formed (Fig. 6).

These traps can be used, in particular, for trapping non-transparent micro-objects inside a ring by allowing a particle to enter the dark region and then closing the trap. Similar experiments were performed by us and are described in Section 5.

4. Dynamic control of contour traps

4.1. Control of trap dimensions

It is obvious that the dimensions of a formed circular trap should depend on the phase delay profile, which has the form of a truncated cone, namely, on the cone width and the phase deflection depth, which can be controlled by changing the

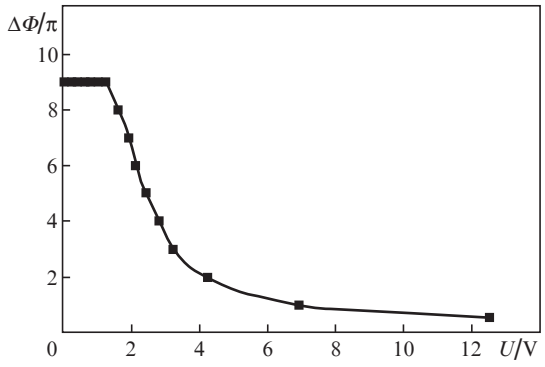

Figure 7. Dependence of the phase delay in an LC layer on voltage amplitude for the experimental sample of LC focusing device.

voltage at the contacts of the LC focusing device. The voltage–phase dependence of the nematic LC layer has a nonlinear character (Fig. 7).

With increasing potential amplitude at the contacts, the voltage drop and, hence, the phase deflection increase, the cone angle decreases and the cone base remains unchanged. This leads to focusing of the light field into a narrower circle at the same distance from the focusing device. As the voltage amplitudes fall into the region of the voltage–phase dependence saturation, the cone base begins to decrease, which leads to a decrease in the distances to the planes of formation of the intensity distribution in the form of circular traps.

Figure 8 presents the calculated light intensity distributions at a distance of 4 cm from the focusing device in the case of simultaneous change of voltage amplitudes at all the four contacts, which demonstrate the possibility of controlling the circle size in a given plane by a corresponding change of potentials at the LC focusing device contacts. One can see that an increase in the potential amplitudes decreases the circle radius. The corresponding dependences of the radius on voltage for different distances from the focusing device to the observation plane are given in Fig. 9.

Note that the circle sizes can be changed very smoothly (theoretically, continuously) due to such an important specific feature of the LC focusing device as the use of a solid electrode for the formation of a voltage distribution in the region of the aperture. This makes it possible to form a smooth continuous phase delay profile and smoothly change the voltage distribution on the focusing device aperture (and,

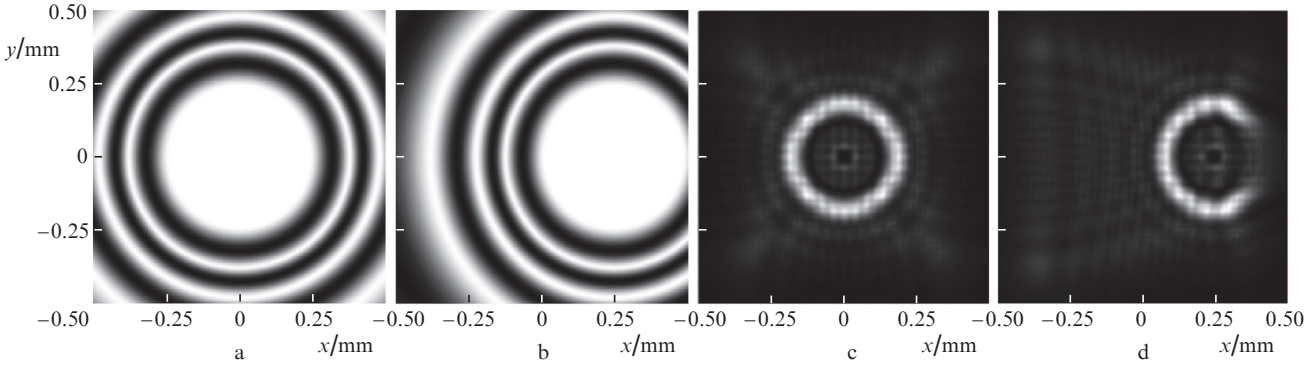

Figure 6. Polarisation interference patterns (a, b) and intensity distributions at a distance of 3 cm from the LC focusing device (c, d). The shifts of distributions are $x_0 = y_0 = 0$ (a, c) and $x_0 = 0.25$ mm, $y_0 = 0$ (b, d).

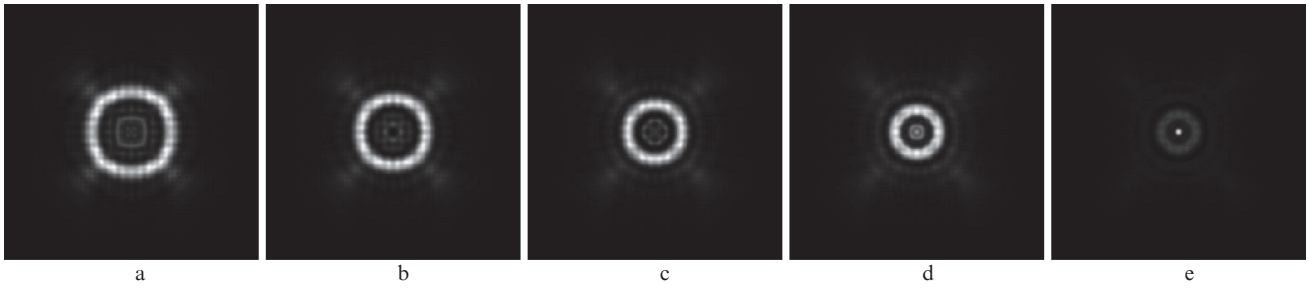

Figure 8. Calculated light intensity distributions at a distance of 4 cm from the focusing device at potential amplitudes at the contacts of 2 (a), 2.2 (b), 2.4 (c), 2.6 (d) and 2.8 V (e).

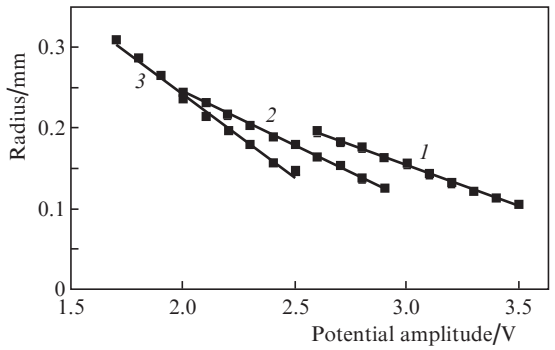

Figure 9. Calculated dependences of a circular trap radius on the voltage at the contacts at distances between the observation plane and the focusing device of 2 (*1*), 3 (*2*) and 4 cm (*3*).

hence, the circle size) by changing the potentials at the contact electrodes. In practice, the possibility of continuous control of the circle size is limited by the discreteness of control voltages.

From the viewpoint of optical trapping, the possibility of controlling the circle size can be rather helpful. For example, the authors of [12] demonstrated the possibility of stable trapping of a transparent (non-absorbing) particle in the dark region of a light circle formed by diffractive optical elements. In this case, the particle size must be slightly larger than the circle radius. Since, for example, biological objects are characterised by variations in their sizes inside a sample, trapping could be optimised by changing the trap parameters (sizes). This is important for trapping both transparent and non-transparent (absorbing) objects in the intensity minimum.

4.2. Control of trap shape

Changing the control voltage parameters, one can change the trap shape from circular to elliptical and vice versa. For example, if it is necessary to transform the voltage distribution so that the equipotential lines in the form of a circle transformed into elliptical lines without a shift of the centre, one must identically change the potential amplitudes at the electrodes of one of the substrates (Fig. 10).

The possibility of smooth control of the shape and size of contour traps can be useful for trapping biological objects of different shapes. For example, elliptical traps make it possible to optimise trapping of erythrocytes, whose shape, as is known, may change from discoidal to spheroidal or dumbbell-like.

4.3. Movement of contour traps

In [7, 8], we showed that, changing the amplitude and/or phase of the potentials applied to the contacts, one can control the position of the circular cone base centre and, therefore, to control the position of a point or contour trap. The

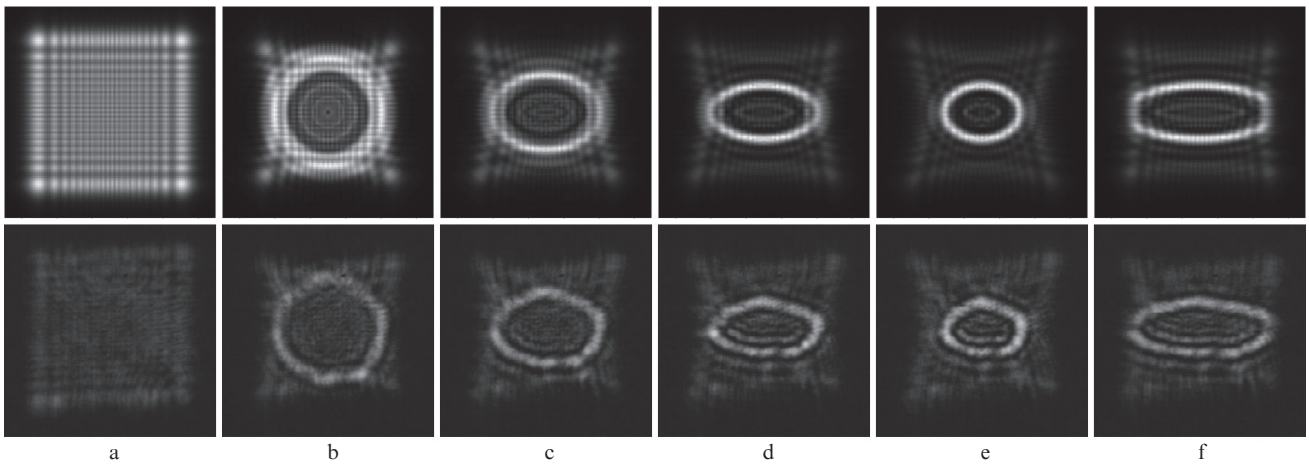

Figure 10. Calculated (upper row) and measured (lower row) light intensity distributions at a distance from the focusing device of 2 cm and the following potential amplitudes at the contacts: $A_{11} = A_{12} = A_{21} = A_{22} = 0$ (a); $A_{11} = A_{12} = 2$ V, $A_{21} = A_{22} = 2$ V (b); $A_{11} = A_{12} = 2$ V, $A_{21} = A_{22} = 2.5$ V (c); $A_{11} = A_{12} = 2$ V, $A_{21} = A_{22} = 3$ V (d); $A_{11} = A_{12} = 2.5$ V, $A_{21} = A_{22} = 3$ V (e); $A_{11} = A_{12} = 1.5$ V, $A_{21} = A_{22} = 3$ V (f).

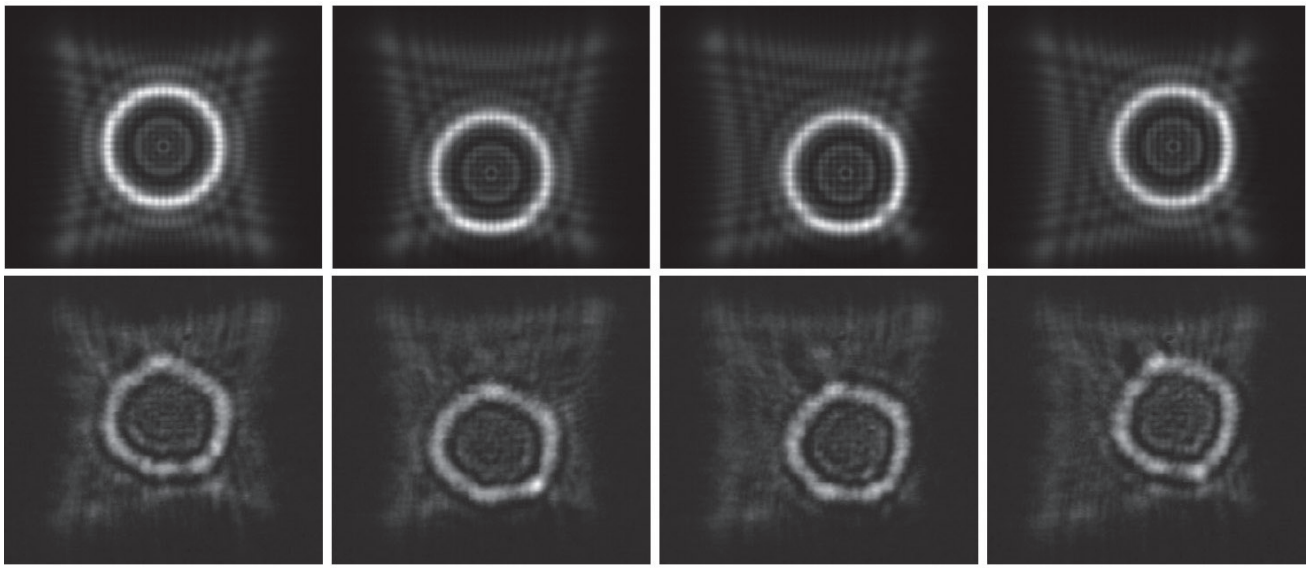

Figure 11. Calculated (upper row) and measured (lower row) light intensity distributions at a distance of 2 cm from the focusing device and the following potential amplitudes at the contacts: $A_{11} = A_{12} = A_{21} = A_{22} = 2.5$ V (a); $A_{11} = A_{12} = 2.5$ V, $A_{21} = 2$ V, $A_{22} = 3$ V (b); $A_{11} = 3$ V, $A_{12} = 2$ V, $A_{21} = 2$ V, $A_{22} = 3$ V (c); $A_{11} = 3$ V, $A_{12} = 2$ V, $A_{21} = A_{22} = 2.5$ V (d).

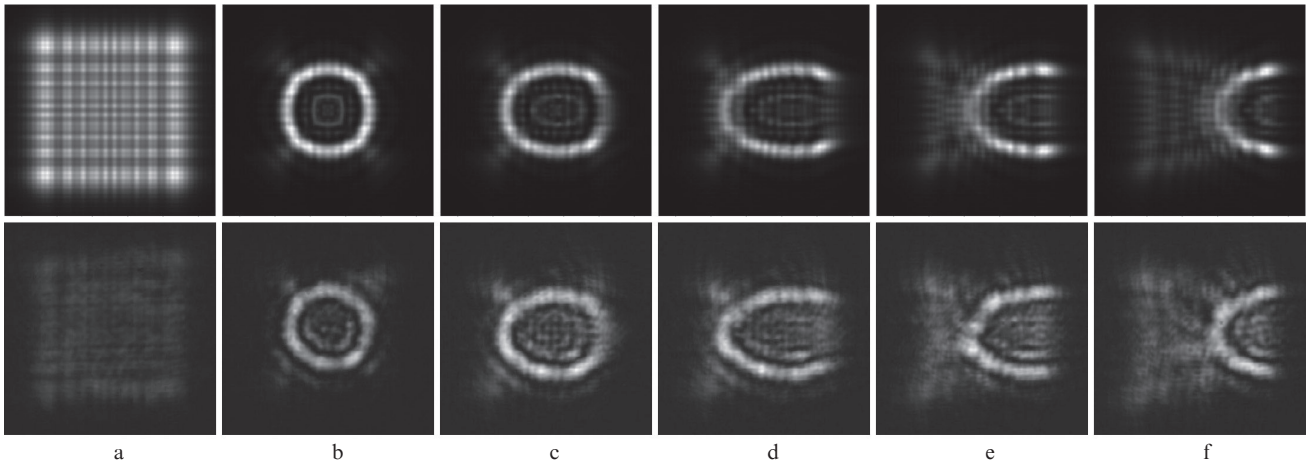

Figure 12. Numerically simulated (upper row) and measured (lower row) light intensity distributions at a distance of 4 cm from the focusing device and the following potential amplitudes at the contacts: $A_{11} = A_{12} = A_{21} = A_{22} = 0$ (a); $A_{11} = A_{12} = A_{21} = A_{22} = 2$ V (b); $A_{11} = 2$ V, $A_{12} = 1.5$ V, $A_{21} = A_{22} = 2$ V (c); $A_{11} = 2$ V, $A_{12} = 1$ V, $A_{21} = A_{22} = 2$ V (d), $A_{11} = 2.5$ V, $A_{12} = 0.5$ V, $A_{21} = A_{22} = 2$ V (e); $A_{11} = 3$ V, $A_{12} = 0$, $A_{21} = A_{22} = 2$ V (f).

results of numerical simulation and experiment shown in Fig. 11 demonstrate the possibility of moving a circle.

Elliptical traps can be moved similarly. In addition, moving elliptical or circular traps, one can form a C-shaped trap and control its shape (Fig. 12).

5. Manipulation experiments

The manipulation experiments were performed using an optical tweezers scheme with the LC focusing device (Fig. 13). The traps were formed with the use of a diode-pumped solid-state laser (0.53 μm). The laser beam was sent through a collimator to the LC focusing device, which formed a required light field distribution in a given plane. Then, the beam was deflected to a 100× objective of a modernised XSP-104 biological microscope, and a minified intensity distribution was

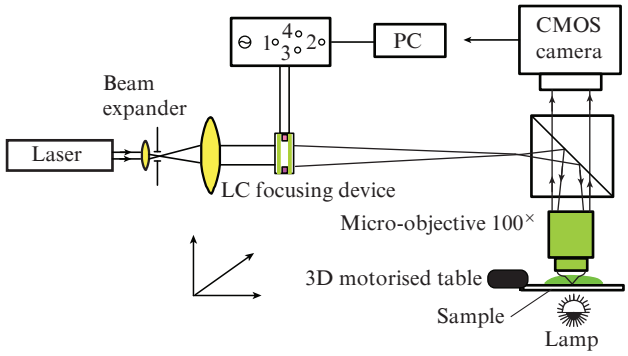

Figure 13. Schematic diagram of laser tweezers based on the LC focusing device.

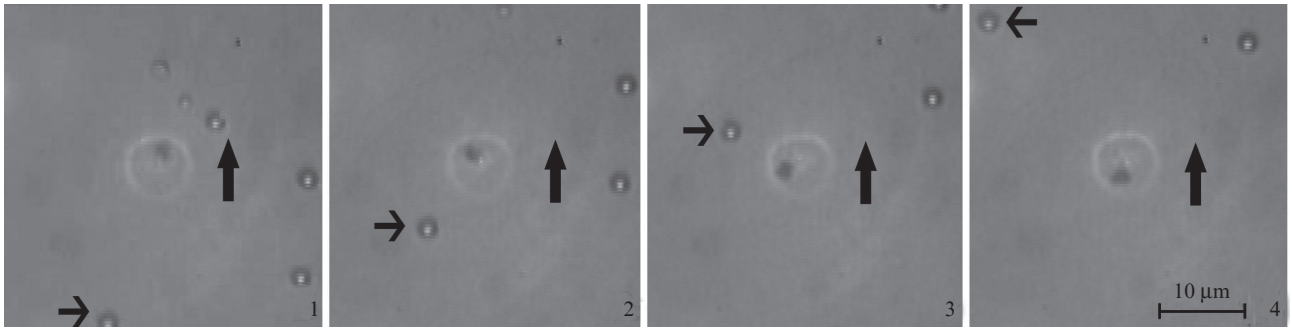

Figure 14. Confinement of an absorbing Al_2O_3 microparticle 1.5 μm in size by a circular trap.

reproduced in the manipulation plane. For visualisation of the observation region of the microscope, a lamp was placed under the cell with micro-objects. The image formed by the microscope was recorded by a DCM-130 digital ocular camera connected to a computer. The focusing device was controlled by a graphical user interface, which allowed us to set the control voltage amplitude and phase at each of the contacts. Using circular light traps formed by the tunable four-channel LC focusing device, we performed experiments on trapping and confinement of absorbing micro-objects – submicron aluminium oxide (Al_2O_3) particles, as well as their conglomerates, suspended in water. The radiation power in the traps was about 10 mW.

For trapping, an absorbing micro-object was drawn near the light trap. Then the radiation was blocked by a shutter and the object was moved to a marker – a virtual vertical line on the screen corresponding to the light circle centre. After this, the shutter was opened and the absorbing particle found itself inside the trap. The experiment on the confinement of an Al_2O_3 microparticle on a moved substrate is illustrated in Fig. 14. The vertical arrow shows the substrate movement direction. The particles outside the trap (marked by the horizontal arrows) move, while the trapped particle remains inside the light circle.

The described experiments were performed both for individual particles with dimensions of 0.5–1.5 μm, which are considerably smaller than the dark region of the circle, and for particle conglomerates with dimensions comparable with those of the minimum intensity region (Fig. 15).

We estimated the maximum substrate movement rates at which the trapped particle is confined by an optical trap. For an absorbing Al_2O_3 particle 1.5 μm in size trapped by a circular optical trap with an outer diameter of 8 μm and a line thickness of 0.9 μm, this rate was 2.5 μm s^{-1} at the radiation power of 10 mW. For comparison, in the case of trapping a transparent latex particle 2.9 μm in diameter by this optical trap, the corresponding rate was 17 μm s^{-1}.

Switching off of a circular trap capturing micro-objects requires additional manipulations with the laser radiation and formation of a virtual marker corresponding to the trap centre. Trapping of particles by a C-shaped trap transforming into a circle after trapping is more convenient and demonstrative. Figure 16 shows photographs illustrating the experiment on trapping and confinement of microparticles by this method. The role of a micro-object is played by an absorbing Al_2O_3 particle about 1.5 μm in size. Micro-objects are moved to a C-shaped trap formed by the focusing device (1). The trap transforms into a circle, and particles find themselves inside the circle (2) and remain there as the substrate moves in the direction shown by the vertical arrow (3, 4).

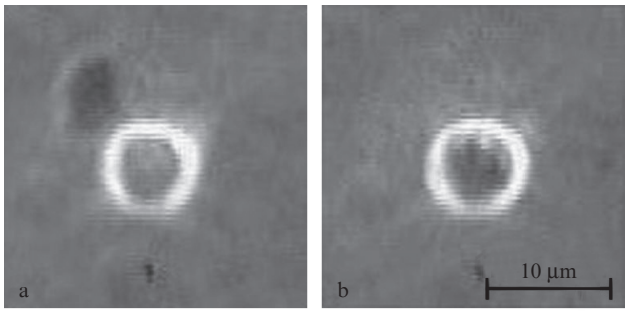

Figure 15. Trapping of a 5–6-μm conglomerate of Al_2O_3 particles by a circular trap: the micro-object is close to the trap (a) and is trapped by it (b).

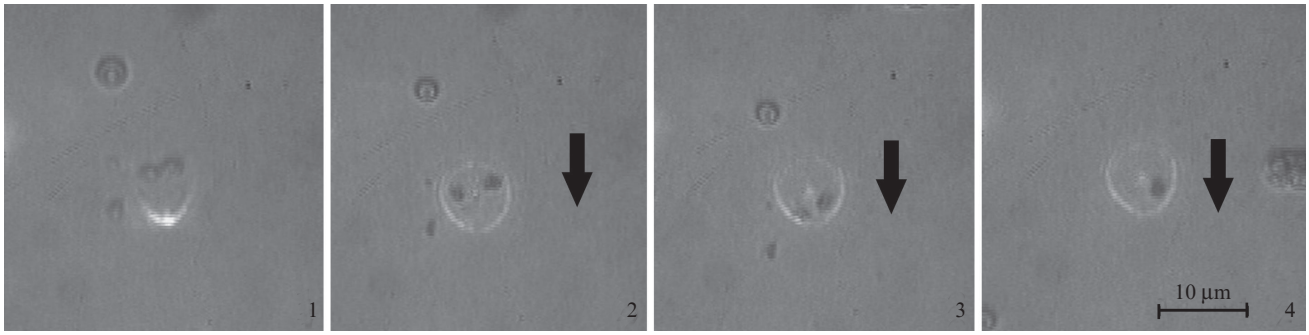

Figure 16. Trapping and confinement of aluminium oxide microparticles 1.5 μm in size by a C-shaped trap transforming into a circle.

The performed experiments clearly demonstrate the principal possibility of using the traps formed by the LC focusing device for optical trapping and confinement of nontransparent particles, as well as for the formation of universal traps for simultaneous trapping of transparent and nontransparent particles. To estimate the trapping efficiency and choose the optimal trap parameters, it is necessary to perform further investigations. Nevertheless, we believe that the studied and described here specific features of the formation and control of contour light fields using the LC focusing device allow us to consider the observed light traps as promising for micromanipulation problems.

6. Conclusions

The possibility of using a four-channel LC focusing device for formation and control of contour optical traps (circular, elliptical and C-shaped) are demonstrated. The considered focusing device operates in the transmission regime, which simplifies its incorporation into an optical tweezers scheme and allows one to make this scheme compact. The experiments were performed at incident power densities up to 30 W cm^{-2}. The use of a solid electrode for the formation of voltage distribution in the region of the aperture makes it possible to form a smooth continuous phase delay profile and continuously change the voltage distribution over the focusing device aperture by changing the potentials at the contact electrodes. This allows one to smoothly change both the size and shape of traps, which was experimentally demonstrated.

The obtained results allow us to suggest that the LC focusing device is promising for application in optical manipulation systems used, for example, in biomedicine.

Acknowledgements. This work was partially supported by the Russian Foundation for Basic Research (Grant No. 14-02-31376mol_a).

References

1. Bowman R., Gibsonand G., Padgett M. *Opt. Express*, **18**, 11785 (2010).
2. Jesacher A., Maurer C., Bernet S., Schwaighofer A., Ritsch-Marte M. *Opt. Express*, **16**, 4479 (2008).
3. Chapin C., Germain V., Dufresne E. *Opt. Express*, **14**, 13095 (2006).
4. Dholakia K., Čižmár T. *Nature Photon.*, **5**, 335 (2011).
5. Padjett M., Bowman R. *Nature Photon*., **5**, 343 (2011).
6. Afanasiev K., Korobtsov A., Kotova S., Losevsky N., Mayorova A., Patlan V., Volostnikov V. *J. Phys.: Conf. Ser*., **414**, 012017 (2013).
7. Kotova S.P., Patlan' V.V., Samagin S.A. *Kvantovaya Elektron*., **41** (1), 58 (2011) [*Quantum Electron*., **41** (1), 58 (2011)].
8. Kotova S.P., Patlan' V.V., Samagin S.A. *Kvantovaya Elektron*., **41** (1), 64 (2011) [*Quantum Electron*., **41** (1), 64 (2011)].
9. Kotova S., Patlan V., Samagin S. *J. Optics*, **15** (3), 035706 (2013).
10. Korobtsov A., Kotova S., Losevsky N., Mayorova A., Patlan V., Samagin S. *J. Optics*, **16**, 035704 (2014).
11. Padjett M., Allen L. *Contempory Phys*., **41** (5), 275 (2000).
12. Dasgupta R., Ahlawat S., Verma R.S., Gupta P.K. *Opt. Express*, **19** (8), 7680 (2011).
13. Daria V.R., Go M.A., Bachor H.-A. *J. Optics*, **13** (4), 044004 (2011).
14. Arlt J., Garces-Chavez V., Sibbett W., Dholakia K. *Opt. Commun*., **197**, 239 (2001).
15. Arlt J., Dholakia K., Soneson J., Wright E. *Phys. Rev. A*, **63**, 063602 (2001).
16. Garces-Chavez V., McGloin D., Melville H., Sibbett W., Dholakia K. *Nature*, **419**, 145 (2002).
17. McGloin D., Garces-Chavez V., Dholakia K. *Opt. Lett*., **28**, 657 (2003).
18. Baumgartl J., Mazilu M., Dholakia K. *Nature Photon*., **2**, 675 (2008).
19. Baumgartl J., Hannappel G.M., Stevenson D.J., Day D., Gu M., Dholakia K. *Lab. Chip*., **9**, 1334 (2009).
20. Siviloglou G., Broky J., Dogariu A., Christodoulides D. *Opt. Photon. News*, **19**, 21 (2008).
21. Porfirev A.P., Skidanov R.V. *Appl. Opt*., **52**, 6230 (2013).
22. Siler M., Jakl P., Brzobohaty O., Zemanek P. *Opt. Express*, **20**, 24304 (2012).
23. Rykov M.A., Skidanov R.V. *Appl. Opt*., **53**, 156 (2014).